International Journal of Minerals, Metallurgy and Materials
Volume 20, Number 11, November 2013, Page 1102
DOI: 10.1007/s12613-013-0840-2

Preparation of metal oxide doped ACNFs and their adsorption performance for low concentration SO_2

Hong-quan Yu, Yan-bo Wu, Tie-ben Song, Yue Li, and Yu Shen

College of Environmental and Chemical Engineering, Dalian Jiaotong University, Dalian 116028, China

(Received: 27 March 2013; revised: 19 May 2013; accepted: 20 May 2013)

Abstract: Metal oxide (TiO_2 or Co_3O_4) doped activated carbon nanofibers (ACNFs) were prepared by electrospinning. These nanofibers were characterized by X-ray diffraction (XRD), scanning electron microscopy (SEM), and Brunner-Emmett-Teller method (BET). The results show that the average diameters of ACNFs were within the range of 200-500 nm, and the lengths were several tens of micrometers. The specific surface areas were 1146.7 m^2/g for TiO_2-doped ACNFs and 1238.5 m^2/g for Co_3O_4-doped ACNFs, respectively. The electrospun nanofibers were used for adsorption of low concentration sulfur dioxide (SO_2). The results showed that the adsorption rates of these ACNFs increased with an increase in SO_2concentration. When the SO_2 concentration was 1.0 μg/mL, the adsorption rates of TiO_2-doped ACNFs and Co_3O_4-doped ACNFs were 66.2% and 67.1%, respectively. The adsorption rate also increased as the adsorption time increased. When the adsorption time was 40 min, the adsorption rates were 67.6% and 69.0% for TiO_2-doped ACNFs and Co_3O_4-doped ACNFs, respectively. The adsorption rate decreased as the adsorption temperature increased below 60 °C, while it increased as the adsorption temperature increased to more than 60°C.

Keywords: activated carbon nanofibers; metal oxides; electrospinning; adsorption; sulfur dioxide

1. Introduction

SO_2, NO_x, and volatile organic compounds (VOCs) are common atmospheric pollutants that are emitted primarily from fossil fuels. Methods have been developed to reduce their emission, such as adsorption, thermal oxidation, biofiltration, and absorption. The adsorption is a preferred technique used for low concentration gaseous pollutant control. Activated carbon (AC) is a general media of adsorption that has been widely used in air purification [1]. In this context, numerous studies [2-7] have tested activated carbon fibers (ACFs), a fabric form of AC, due to their unique characteristics, e.g., large specific surface area, uniform pore size distribution (PSD), and amenability to surface functionalization [2-7]. Recent studies have shown that commercial ACFs impregnated with metals/metal oxides [8-11] or surface-functionalized with a suitable reagent [12] are more efficient with respect to the catalytic oxidation of SO_2, NO, and VOCs. Recently, a type of activated carbon nanofibers (ACNFs) demonstrated significant applications on elimination of toxic gases or liquids, production of cells and capacitors due to light weight, high large specific surface area, and microporous structure [13-15]. This material can adsorb contaminants more efficiently than ACFs alone or ACFs impregnated with metals [16-17]. Electrospun fibers have high specific surface area, high aspect ratio, and dimensional stability; hence, ACNFs with the high specific surface area, large micropore volume, and narrow micropores can be prepared from electrospun fibers at the optimal activation temperature. However, little attention has been paid on studying the adsorption capacity of electrospun ACNFs [18-19].

Embedding metals and metal oxides in a precursor would increase the gas and liquid adsorption capacity of the resulting composite ACNFs [20], because metal and metal oxide nanoparticles could increase the specific surface area and pore volume by their catalytic activity during the precursor pyrolysis [21-24]. It is worth mentioning that as far as gas and liquid adsorption capacity of composite ACNFs is concerned, metal oxides always show superiority over metals due to the high thermal stability at elevated temperatures [20, 25-26]. Oh *et al.* [27] found that em-

Corresponding author: Hong-quan Yu E-mail: yuhq7808@djtu.edu.cn

bedding manganese nanoparticles in the precursor would enhance the specific surface area and pore volume that would lead to a higher toluene adsorption capacity. Im *et al.* [20] observed and reported different pore structures of ACNFs containing Fe, Mg, Fe_3O_4, and CuO embedded in the precursor, which was related to the nature of metals and metal oxides embedded in ACNFs. Im *et al.* [28] also found that vanadium pentoxide embedded in the precursor of ACNFs acted as a catalyst; and the resulting dissociated oxygen generated the ultra-micropores through the formation of CO and CO_2 during pyrolysis. This would increase the hydrogen adsorption capacity of ACNFs, which were used as the hydrogen storage medium. Kim and Lim [21] demonstrated that the acetaldehyde adsorption capacity of ACNFs containing TiO_2 nanoparticles embedded in the precursor was a function of the surface area. Nataraj *et al.* [22] showed that using nickel nitrate in polyacrylonitrile (PAN) as a precursor, even at a low dosage ($\leqslant$ 1wt%), can remarkably increase the specific surface area, pore volume, and mean pore size of the resultant composite ACNFs.

In our research, the composite nanofibers of polyv inylpyrrolidone (PVP, molecular weight M_w = 1300000) and tetrabutyl titanate (TBT), as well as PVP/cobalt acetate composite nanofibers, were prepared by electrospinning. These nanofibers were processed by preoxidation, carbonation, and activation to obtain metal oxide (TiO_2 or Co_3O_4) doped ACNFs. These metal oxide doped ACNFs were used to adsorb SO_2 at low concentration. The adsorption effect was demonstrated as a function of SO_2 concentration, adsorption temperature, and time. Experiment results showed that the adsorption performance of Co_3O_4-doped ACNFs was better than TiO_2-doped ACNFs, due to specific surface area and total pore volume.

2. Methods

In order to prepare TiO_2-doped ACNFs, 1.5 mL TBT solution were dropped to 8wt% PVP ethanol solution, followed by constant stirring in a water bath at 50°C for 4 h, and the final electrospinning solutions were obtained. The schematic diagram of the electrospinning setup is shown in Fig. 1, which consists of three major parts: a high-voltage power supply, a spinneret (plastic needle), and a collector (rotating plastic drum). In this electrospinning process, the solution was pumped through a nozzle to a collector at high voltage to form an electrically charged jet. The solution jet was solidified on the collector with the evaporation of solvent. In this experiment, the applied voltage was 12 kV, and the collection distance was 20 cm. Rotating speeds of the drum were set to 200 r/min corresponding to linear speed 0.5 m/s. The PVP/TBT fibers were dried initially for 8 h at room temperature under vacuum and preoxidated at 250°C for 1 h. Then, the PVP/TBT fibers were annealed by heating from room temperature to 500°C at a rate of 1°C/min in N_2 stream and kept for 1 h at 500°C to carbonize. The carbonized PVP/TBT fibers were immersed in 1 mol/L HNO_3 solution for 12 h. These fibers were activated in N_2 atmosphere by "temperature-programming" and kept for 1 h at 600°C. Finally, TiO_2-doped ACNFs were obtained. Co_3O_4-doped ACNFs were also prepared under the same experimental conditions using cobalt acetate and PVP. These metal oxides (TiO_2 or Co_3O_4) doped ACNFs were used to adsorb low concentration SO_2 under different adsorption conditions, including the concentration of SO_2, adsorption temperature, and adsorption time.

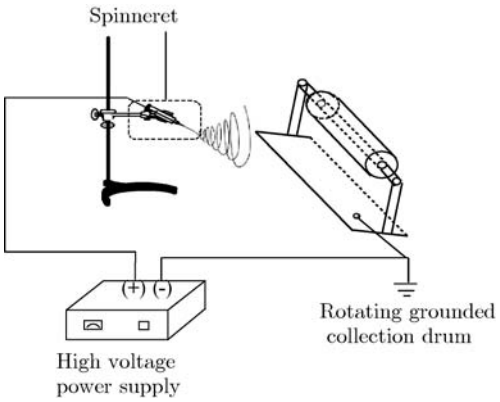

Fig. 1. Schematic diagram of the electrospinning setup.

The morphology of these metal oxide doped ACNFs were examined on Hitachi JSM-6360(LV) scanning electron microscopy (SEM, Hitachi, Japan) at 20 kV. The X-ray diffraction (XRD) patterns were obtained on a Rigaku D/max-rA X-ray diffractometer (Rigaku, Japan) with Cu target radiation source (λ = 0.15405 nm). The specific surface areas were calculated by the standard Brunner-Emmett-Teller (BET) equation that was applied to the experimental adsorption isotherm over a relative pressure range of 0.05 to 0.30. The adsorption isotherms were measured by Quanta chrome NOVA 2000 (Quanta chrome, US) with nitrogen at 77 K.

3. Results and discussion

3.1. Characterization of morphology and structure

Fig. 2 shows the SEM images of PVP/TBT and PVP/cobalt acetate composite fibers, which present smooth surfaces and uniform distributed diameter. For PVP/TBT composite fibers, the diameter range is 200-400 nm; while for PVP/cobalt acetate composite fibers, the diameter range is 300-500 nm. These fibers are rough in surface and do not obviously change in terms of diameter after being carbonized.

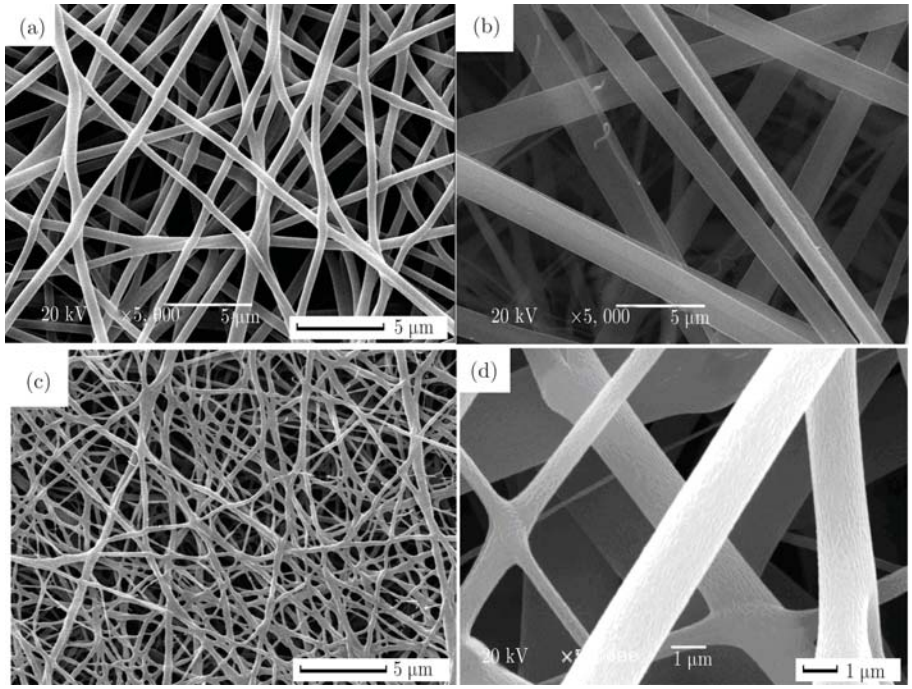

Fig. 2. SEM images of PVP/TBT (a) and PVP/cobalt acetate (b) composite fibers prepared by electrospining method. SEM images of PVP/TBT (c) and PVP/cobalt acetate (d) composite fibers carbonized in N_2 atmosphere.

Fig. 3 shows the XRD patterns of PVP/TBT and PVP/cobalt acetate composite nanofibers after carbonation. In Fig. 3(a), the peaks appearing at 25.08°, 37.72°, 47.68°, 55.35°, and 62.64° belong to anatase TiO_2 (JCPDS card No. 71-1169). In Fig. 3(b), the characteristic peaks appearing at 31.24°, 36.81°, 44.82°, 59.28°, and 65.26° belong to Co_3O_4 (JCPDS card No. 71-1169). No additional phase is formed in this pattern. These results indicate that the PVP/TBT and PVP/cobalt acetate composite nanofibers contain $TiO_2$and Co_3O_4, respectively, after carbonation.

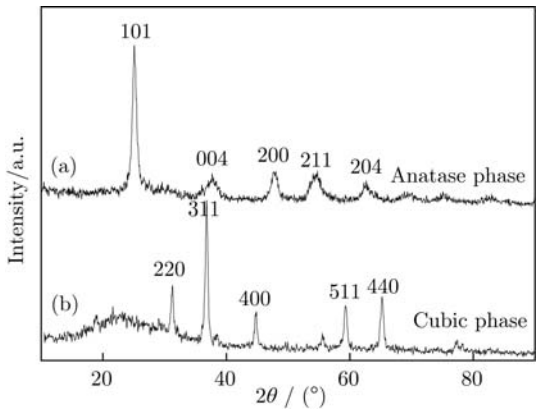

Fig. 3. XRD patterns of PVP/TBT (a) and PVP/cobalt acetate (b) composite fibers carbonated at 500°C.

3.2. Specific surface area and pore volume of metal oxide doped ACNFs

The data of surface area and pore volume of TiO_2-doped ACNFs and Co_3O_4-doped ACNFs are given in Table 1. For TiO_2doped ACNFs, the surface area, total pore volume, micropore volume, and mesopore volume are 1146.7 m^2/g, 0.5028 cm^3/g, 0.4966 cm^3/g, and 0.0062 cm^3/g, respectively. For Co_3O_4-doped ACNFs, the specific surface area, total pore volume, micropore volume, and mesopore volume are 1238.5 m^2/g, 0.5637 cm^3/g, 0.5525 cm^3/g, and 0.0112 cm^3/g, respectively. The micropore volume proportion is about 98.8% of the total pore volume in the ACNFs. It suggests that Co_3O_4-doped ACNFs has a bigger specific surface area and a more pore volume than TiO_2-doped ACNFs, and the adsorption performance of Co_3O_4-doped ACNFs would be better than that of TiO_2-doped ACNFs.

Table 1. Surface area and pore volume of metal oxide doped ACNFs

Samples	Specific surface Area/$(m^2 \cdot g^{-1})$	Total pore volume/$(cm^3 \cdot g^{-1})$	Micropore volume/$(cm^3 \cdot g^{-1})$	Mesopore volume/$(cm^3 \cdot g^{-1})$
TiO_2 doped ACNFs	1146.7	0.5028	0.4966	0.0062
Co_3O_4 doped ACNFs	1238.5	0.5637	0.5525	0.0112

3.3. Adsorption performance of metal oxide doped ACNFs for low concentration SO_2

The metal oxide doped ACNFs were used to study the performance of low concentration SO_2 adsorption. The adsorption rates of these ACNFs vary with SO_2 concentration as shown in Fig. 4. It illustrates that the adsorption rates increase as the SO_2 concentration increases. However, the adsorption rates are nearly constant when the SO_2 concentrations are more than 0.8 μg/mL. When the SO_2 concentration is 1.0 μg/mL, the adsorption rates of TiO_2-doped ACNFs and Co_3O_4-doped ACNFs are 66.2% and 67.1%, respectively, which indicates that the adsorption rate of Co_3O_4-doped ACNFs is larger than that of TiO_2-doped ACNFs.

Fig. 5 shows the relationship between the adsorption rate of different samples and adsorption time. It is shown that the adsorption rate increases when the adsorption time increases. The adsorption rates of TiO_2-doped ACNFs and Co_3O_4-doped ACNFs are 67.6% and 69.0% with an adsorption time of 40 min, respectively, which do not reach the adsorption saturation. This may be caused by deficient driving force and low SO_2 concentration.

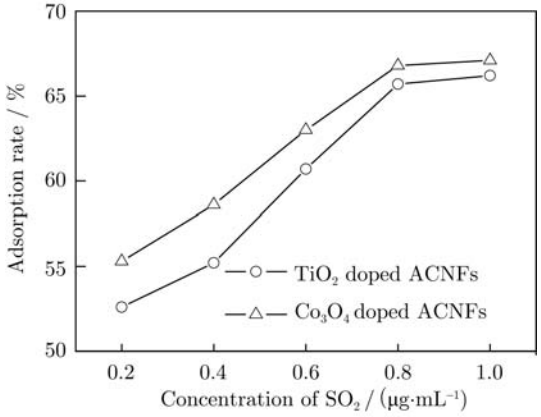

Fig. 4. Adsorption rate of ACNFs with different SO_2 concentrations at room temperature with an adsorption time of 10 min and an SO_2 flow rate of 20 mL/min.

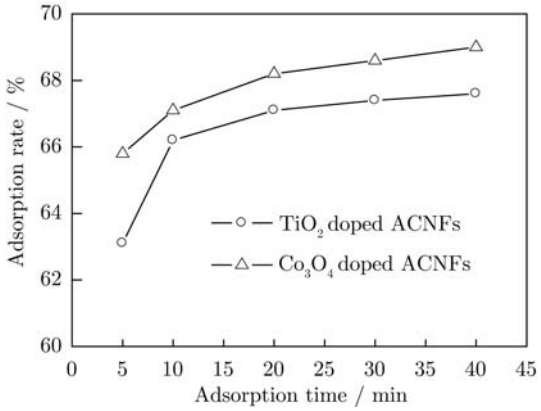

Fig. 5. Adsorption rate of ACNFs with different adsorption time intervals with an SO_2 concentration of 1.0 μg/mL and an SO_2 flow rate of 20 mL/min.

The relationship between adsorption rate and temperature with respect to different metal oxide doped ACNFs is shown in Fig. 6. The adsorption rate decreases with an increase in temperature when the temperature is below 60°C, while it increases when the temperature is more than 60°C. According to the results, it can be concluded that low temperature may be helpful for SO_2 adsorption on ACNFs surfaces because the reaction of SO_2 and O_2 generating SO_3 is an exothermic reaction, whereas the upturn of adsorption rate would be attributed to rapid generation of SO_3 from SO_2 and O_2 when the temperature was more than 60°C.

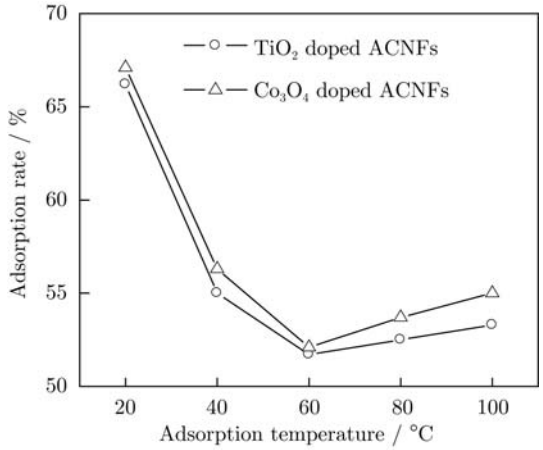

Fig. 6. Adsorption rate of ACNFs with different adsorption temperatures with an SO_2 concentration of 1.0 μg/mL, an adsorption time of 10 min, and an SO_2 flow rate of 20 mL/min.

4. Conclusion

Metal oxide doped ACNFs were prepared by an electrospinning method, with the average diameters of 200-500 nm and the lengths of several tens of micrometers. Their micropore volume proportion is both 98.8% of the total pore volume. The specific surface area of these ACNFs is 1146.7 m^2/g for TiO_2-doped ACNFs and 1238.5 m^2/g for Co_3O_4-doped ACNFs, respectively. The ACNFs were used to adsorb low concentration SO_2. The results indicate that adsorption temperature, adsorption time, and SO_2 concentration are parameters that impact the adsorption rate of SO_2. High SO_2 concentration, low temperature, and long time are helpful for the adsorption of SO_2.

Acknowledgements

This work was financially supported by the National Natural Science Foundation of China (Nos. 50802010, 50972021, 21076028, and 61078061) and the Program

for Liaoning Excellent Talents in Universities (No. LJQ2011047).

References

[1] R.H. Bradley and B. Rand, On the physical adsorption of vapors by microporous carbons, *J. Colloid Interf. Sci.*, 169(1995), No. 1, p. 168.

[2] M. Suzuki, Activated carbon fiber: fundamentals and applications, *Carbon*, 32(1994), No. 4, p. 577.

[3] I. Mochida, Y. Korai, M. Shirahama, S. Kawano, T. Hada, Y. Seo, M. Yoshikawa, and A. Yasutake, Removal of SO_x and NO_x over activated carbon fibers, *Carbon*, 38(2000), No. 2, p. 227.

[4] Z.H. Huang, F.Y. Kang, Y.P. Zheng, J.B. Yang, and K.M. Liang, Adsorption of trace polar methy-ethyl-ketone and non-polar benzene vapors on viscose rayon-based activated carbon fibers, *Carbon*, 40(2002), No. 8, p. 1363.

[5] S. Adapa, V. Gaur, and N. Verma, Catalytic oxidation of NO by activated carbon fiber (ACF), *Chem. Eng. J.*, 116 (2006), No. 1, p. 25.

[6] V. Gaur, A. Sharma, and N. Verma, Preparation and characterization of ACF for the adsorption of BTX and SO_2, *Chem. Eng. Process.*, 45(2006), No. 1, p. 1.

[7] V. Gaur, R. Asthana, and N. Verma, Removal of SO_2 by activated carbon fibers in the presence of O_2 and H_2O, *Carbon*, 44(2006), No. 1, p. 46.

[8] V. Gaur, A. Sharma, and N. Verma, Catalytic oxidation of toluene and *m*-xylene by activated carbon fiber impregnated with transition metals, *Carbon*, 43(2005), No. 15, p. 3041.

[9] V. Gaur, A. Sharma, and N. Verma, Removal of SO_2 by activated carbon fibre impregnated with transition metals, *Can. J. Chem. Eng.*, 85(2007), No. 2, p. 188.

[10] J.Y. Wang, F.Y. Zhao, Y.Q. Hu, R.H. Zhao, and R.J. Liu, Modification of activated carbon fiber by loading metals and their performance on SO_2 removal, *Chin. J. Chem. Eng.,* 14(2006), No.4, p.478.

[11] P. Lu, C.T. Li, G.M. Zeng, L.J. He, D.L. Peng, H.F. Cui, S.H. Li, and Y.B. Zhai, Low temperature selective catalytic reduction of NO by activated carbon fiber loading lanthanum oxide and ceria, *Appl. Catal. B,* 96(2010), No. 1-2, p. 157.

[12] R.S. Rathore, D.K. Srivastava, A.K. Agarwal, and N. Verma, Development of surface functionalized activated carbon fiber for control of NO and particulate matter, *J. Hazard. Mater.*, 173(2010), No. 1-3, p. 211.

[13] D. Esrafilzadeh, M. Morshed, and H. Tavanai, An investigation on the stabilization of special polyacrylonitrile nanofibers as carbon or activated carbon nanofiber precursor, *Synth. Met.*, 159(2009), No. 3-4, p. 267.

[14] J.S. Im, S.J. Park, T. Kim, and Y.S. Lee, Hydrogen storage evaluation based on investigations of the catalytic properties of metal/metal oxides in electrospun carbon fibers, *Int. J. Hydrogen Energy*, 34(2009), No. 8, p. 3382.

[15] J. Zhu, A. Holmen, and D. Chen, Carbon nanomaterials in catalysis: proton affinity, chemical and electronic properties, and their catalytic consequences, *ChemCatChem,* 5 (2013), No. 2, p. 378.

[16] R.M. Singhal, A. Sharma, and N. Verma, Micro-nano hierarchal web of activated carbon fibers for catalytic gas adsorption and reaction, *Ind. Eng. Chem. Res.*, 47(2008), No. 10, p. 3700.

[17] A.K. Gupta, D. Deva, A. Sharma, and N. Verma, Adsorptive removal of fluoride by micro-nanohierarchal web of activated carbon fibers, *Ind. Eng. Chem. Res.,* 48(2009), No. 21, p. 9697.

[18] K.S. Yang, Y.J. Yoon, M.S. Lee, W.J. Lee, and J.H. Kim, Further carbonization of anisotropic and isotropic pitch-based carbons by microwave irradiation, *Carbon*, 40 (2002), No. 6, p. 897.

[19] B. Cagnon, X. Py, A. Guillot, and F. Stoeckli, The effect of the carbonization/activation procedure on the microporous texture of the subsequent chars and active carbons, *Microporous Mesoporous Mater.*, 57(2003), No.3, p.273.

[20] J.S. Im, S.J. Park, T. Kim, and Y.S. Lee, Hydrogen storage evaluation based on investigations of the catalytic properties of metal/metal oxides in electrospun carbon fibers, *Int. J. Hydrogen Energy*, 34(2009), No. 8, p. 3382.

[21] S. Kim and S.K. Lim, Preparation of TiO_2-embedded carbon nanofibers and their photocatalytic activity in the oxidation of gaseous acetaldehyde, *Appl. Catal. B*, 84(2008), No. 1-2, p. 16.

[22] S.K. Nataraj, B.H. Kim, J.H. Yun, D.H. Lee, T.M. Aminabhavi, and K.S. Yang, Effect of added nickel nitrate on the physical, thermal and morphological characteristics of polyacrylonitrile-based carbon nanofibers, *Mater. Sci. Eng. B,* 162(2009), No. 2, p. 75.

[23] A. Oya, S. Yoshida, J. Alcaniz-Monge, and A. Linares-Solano, Formation of mesopores in phenolic resin-derived carbon fiber by catalytic activation using cobalt, *Carbon*, 33(1995), No. 8, p. 1085.

[24] C. Tekmen, Y. Tsunekawa, and H. Nakanishi, Electrospinning of carbon nanofiber supported Fe/Co/Ni ternary alloy nanoparticles, *J. Mater. Process. Technol.,* 210(2010), No. 3, p. 451.

[25] R.K. Dwivedi and G. Gowda, Thermal stability of aluminium oxides prepared from gel, *J. Mater. Sci. Lett.*, 4(1985), No. 3, p. 331.

[26] J.D. Nowak and C.B. Carter, Forming contacts and grain boundaries between MgO nanoparticles, *J. Mater. Sci.*, 44(2009), No. 9, p. 2408.

[27] G.Y. Oh, Y.W. Ju, H.R. Jung, and W.J. Lee, Preparation of the novel manganese-embedded PAN-based activated carbon nanofibers by electrospinning and their toluene adsorption, *J. Anal. Appl. Pyrol.*, 81(2008), No. 2, p. 211.

[28] J.S. Im, O. Kwon, Y.H. Kim, S.J. Park, and Y.S. Lee, The effect of embedded vanadium catalyst on activated electrospun CFs for hydrogen storage, *Microporous Mesoporous Mater.*, 115(2008), No. 3, p. 514.